

PRESSURE RESISTANT BULKHEAD PENETRATORS FOR FIBER OPTICS IN DEEP OCEAN APPLICATIONS

**Steven J. Cowen
Ocean Technology Department
Naval Ocean Systems Center
San Diego, California 92152**

ABSTRACT

This paper describes results obtained at the Naval Ocean Systems Center, San Diego, under Independent Exploratory Development funding. The objective was to develop a robust, fully-demountable, high pressure penetrator design suitable for coupling light signals transmitted by optical fiber elements in an undersea cable operated at high ambient hydrostatic pressure into an electronics package or manned space. The feasibility of constructing such penetrators utilizing Graded Refractive INDEX (GRIN) rod lenses as combination pressure barriers and imaging devices was demonstrated. Prototype realizations exhibited excellent optical throughput performance and readily survived in excess of 10,000 psi pressure differential as well as tolerating a wide temperature range. The design lends itself to hermetic construction for applications requiring no vapor diffusion over long mission durations. Such devices exhibit excellent potential for satisfying SUBSAFE requirements for manned submersible applications.

INTRODUCTION

Watertight optical interfacing devices will be required in order to realize practical underwater systems employing fiber optic cables for command, control, and communications. Optical penetrators may also be required in systems utilizing optical fibers as sensors. Because the penetrator provides the means by which the optical signals carried by the fiber optic elements are transferred between the high hydrostatic pressure environment of the cable and the low pressure environment of the electronics package or manned portion of an underwater system, it is a key component required in practically all proposed fiber optic applications under the ocean.

A viable and flexible fiber optic penetrator design would incorporate many features which have historically evolved in the case of presently available electrical penetrators. Unless these proven features are supported, undesirable system impacts might occur which would negate many of the advantages inherent with fiber optic cables compared to their coaxial cable counterparts.

- The penetrator design should exhibit low optical light loss. Insertion loss characteristics should be comparable to, and at least as repeatable as, the better optical fiber connectors presently available in the marketplace. The optical characteristics should be maintained over the entire spectral region utilized for communications.
- The penetrator design should lend itself to efficient certification procedures. It should be possible to test and certify the pressure-integrity function of the device at the time of manufacture--prior to integration with the cable and optoelectronics. Ideally, the pressure barrier subcomponent should be standardized and type certified. It should lend itself to integration with any type of optical fiber or connector when incorporated into the final penetrator configuration.
- The penetrator-to-cable interface should be fully demountable from both the high and low pressure sides of the bulkhead (i.e., connectorized). Ideally, the high pressure side should be capable of underwater make/break operation, a valuable asset for some important system applications. Full demountability obviates the requirement for treating the penetrator, the optoelectronics assembly and the cable as a single unit. It allows separation for the purpose of repair, exchange, transport, and storage of the individual subsystems over the life and mission profile of the system.
- The design should be compatible with a wide variety of optical fiber types and optical connector styles. This reduces the certification burden as well as minimizes inventory requirements. One generic penetrator type should be capable of operation with a wide variety of optical fiber sizes and fiber optic connector styles via a standardized, type-accepted body.
- The design should be inherently straightforward to manufacture in a repeatable fashion while maintaining reasonable manufacturing tolerances. It should not be so complex that reliability and cost-effectiveness are compromised.
- The design should be rugged and robust, permitting operation over a wide range of temperature and pressure conditions. It should be resistant to damage by vibration

and explosive shock. Overall system performance must not be compromised in any way due to limitations of the fiber optic penetrator.

- The design should lend itself to hermetic construction for applications requiring sustained exposure to high hydrostatic pressures. For reliability, the design should resist vapor intrusion. Glass-to-metal or glass-to-ceramic seals should be incorporable so as to form a hermetic vapor barrier without requiring a major redesign or recertification effort.

Historically, epoxy-filled hypodermic needles, epoxy pottings, and elastomeric squeeze bushings (references 1 and 2) have been employed when it is required to transfer light from an optical fiber across a pressure gradient. These techniques all realize their light transfer function by means of physically sealing to the external cable sheath or to the optical fiber itself. Such approaches fail to satisfy all or most of the criteria describing a viable penetrator realization as stated above. While sometimes serving as adequate solutions when applied to test and evaluation of developmental fiber optic components, reliance upon these techniques is unrealistic and would result in undesirable engineering and operational compromises if applied to Navy system applications.

This paper reports a prototype penetrator design potentially capable of satisfying all of the above requirements. We believe it represents an important first step toward realizing workable high pressure fiber optic penetrators for future Navy and commercial applications employing fiber optic cables.

REALIZATION

The penetrator realization reported here is based upon the concept disclosed in reference 3. This approach utilizes a GRIN rod lens of nominally one half pitch length as a combination pressure barrier and imaging device, schematically depicted in Figure 1. A GRIN lens is a glass rod whose bulk properties result in optical imaging of light in a manner analogous to conventional, curved lenses. Prototype, demountable penetrator units developed at NOSC, utilizing the one-half pitch GRIN lens window concept, combined with refinements relating to positional rod location and connector transverse alignment, exhibit approximately 1 - 1.5 dB of optical insertion loss, making them optically comparable to many of the better fiber optic connectors themselves. Intrinsic insertion loss of the GRIN lens is on the order of 0.3 dB; this permits a very low level of insertion loss to be realized in nondemountable designs. Prototype penetrators have been tested to hydrostatic pressures in excess of 10,000 psi (corresponding to depths commensurate with over 95% of the ocean floor) without failure. No degradation in optical performance was observed after high pressure “soaks” lasting several days; this indicated that inconsequential positional creep in rod position was taking place due to long-term applied

stress. Temperature cycling over a range from -40 C to +100 C caused no glass spalling due to mismatch of temperature coefficients between glass and metal. A photograph of a prototype fiber optic penetrator is shown in Figure 2.

OPTICAL CONSIDERATIONS

The GRIN rod lens was the SELFOC Type SLS/2mm manufactured by the Nippon Sheet Glass Company of Japan and distributed by the NSG USA. The units available in 1980 exhibited the following characteristics:

Numerical Aperture (NA)	0.30
On-axis Refractive Index (n_s)	1.545
Radial Grading Constant (A)	0.0361
Nominal Diameter	2.0 mm
Nominal Pitch Length	32.8 mm
Cost in 1980, Unit Quantities	\$40

The type SLS GRIN lens appears to be the best choice among SELFOC products in that it exhibits adequate numerical aperture to collect nearly all the light emitted from a low-loss, graded index optical fiber (whose NA typically ranges from 0.14 to 0.28). Relatively moderate chromatic pitch dependence is inherent in the Type SLS compared to larger NA devices such as the Type SLW. This is very important in the case of wavelength duplexed communications link applications. Two millimeters corresponds to the largest standard diameter presently available in the SELFOC line, although larger diameter lenses have been fabricated and are currently being transitioned into production. Larger diameter lenses minimize the mechanical interfacing mismatch of lens to connector, facilitating fabrication. Likewise, ultra-high resolution SELFOC lenses have been developed which permit imaging of single mode optical fibers with low loss. The device employed to construct the penetrators reported here is a standard item currently being mass-produced in Japan - mass production keeps reproducibility high and cost low.

Referring to Figure 3, equations (1) and (2) describe the imaging rules of a SELFOC lens, modified for the case where the device is immersed in a matching fluid medium.

$$\ell_1 = \frac{n}{n_s \sqrt{A}} \frac{n_s \ell_2 \sqrt{A} \cos \sqrt{AZ} + n \sin \sqrt{AZ}}{n_s \ell_2 \sqrt{A} \sin \sqrt{AZ} - n \cos \sqrt{AZ}} \quad (1)$$

$$P = \frac{\sqrt{AZ}}{2\pi} \quad (2)$$

where: ℓ_1, ℓ_2 = Image plane positions, mm

Z = Length of SELFOC lens, mm

A = SELFOC lens radial grading constant

n_s = Refractive index of the SELFOC lens on the optical axis

n = Refractive index of the medium surrounding the SELFOC lens

P = SELFOC lens fractional pitch length

If the SELFOC lens is chosen to be exactly one-half pitch length, an object in contact with one face creates an inverted, real image of itself (at unity magnification) on the opposite face. This would be undesirable in a practical penetrator because of the possibility of entrapping grit between the lens face and the connector end, scratching both the lens and the fiber held by the connector. A small setback between lens face and connector, implying that imaging should occur slightly outside of the SELFOC lens, is desirable. As determined by equations 1 and 2, this requires that the lens length be slightly less than one-half pitch.

Equations (1) and (2) are plotted in Figure 4 for the case of symmetrical lens-to-connector spacing conditions where the rod lens is immersed in an oil medium having a refractive index of 1.50.

It is noted that a locus of conjugate spacing ($L = \ell_1 = \ell_2$) occurs which is relatively linear over the dimensions of interest, 25 - 100 micrometer (0.001 - 0.004 inch). In this region, the required pitch length can be quickly determined by employing a linear regression approximation as expressed by equation (3).

$$L = 11210 - 22419P \quad (3)$$

where:

L is in micrometers, and

P is the SELFOC lens fractional pitch length

For example, in order to achieve a 38.1 micrometer clearance dimension between lens face and connector (0.0015 inch) a lens fractional pitch length of 0.4983 is dictated.

Because the refractive index of all transparent materials is a function of wavelength and because SELFOC lenses are composed of a glass composite (thallium-doped borosilicate in the case of the Type SLS), the pitch length of a given lens is a function of wavelength. This implies that the clearance dimensions calculated above depend upon the wavelength of light transmitted through the lens. In the case of wavelength multiplexed or duplexed transmission schemes, the lens face to connector standoff dimension can only be “correct” at one wavelength. It is necessary in such cases to predict the performance degradation expected insofar as insertion loss is concerned.

The pitch length of a SELFOC lens is given by equation (4) and wavelength dependence of the glass composing the Type SLS lens by equations (5a and 5b).

$$z = \sqrt{2\pi PR} \sqrt{\frac{n_o(\lambda)}{\Delta n(\lambda)}} \quad (4)$$

$$n_o = 1.5345 + 7.40 \times 10^5/\lambda^2 \quad (5a)$$

$$n_r = 1.5076 + 5.00 \times 10^5/\lambda^2 \quad (5b)$$

where:

R = Radius of SELFOC lens, mm

λ = Optical wavelength in Å

Δn = $n_o(\lambda) - n_r(\lambda)$

Plotting dP/P as a function of wavelength, Figure 5 is obtained. The percentage change in pitch length is normalized to a wavelength separation of 1 micron (10,000 Å).

It is observed that the change in effective pitch length as a function of wavelength is substantial at short wavelengths (i.e., the visible portion of the spectrum) but much less pronounced in the near infrared. For example, in the case where the two wavelengths are 0.83 micron and 1.06 microns, as in a typical wavelength multiplexed communications link, a SELFOC rod exhibiting 0.499 pitch characteristics at the short wavelength has an effective pitch length of only 0.491 at the long wavelength. This result will be utilized later in this paper to predict the increase in insertion loss which would be exhibited by a

penetrator employed under such conditions. Because the trend in high performance fiber optic systems is toward longer wavelengths where optical fiber transmission characteristics are optimized, the example considered above represents a worst-case situation. For example: if the two wavelengths are changed to 1.27 microns and 1.55 microns (corresponding to the high optical performance spectral windows observed in modern optical fibers), the effective pitch lengths become 0.498 at the short wavelength and 0.496 at the long wavelength. Put another way, the SELFOC rod characteristics appear more nearly achromatic as the wavelengths are shifted farther into the infrared. This is fortunate in that it simultaneously optimizes the data transmission characteristics of the optical fiber as well.

Several SELFOC lenses were evaluated to determine optical insertion loss when conjugately imaging 50 micrometer core, graded index optical telecommunication fibers as is depicted in Figure 6.

The optical fiber was typical of low-loss, graded index optical waveguide employed for high bandwidth telecommunications. It exhibited a numerical aperture of 0.22 and an attenuation of 3 dB/Km at a wavelength of 0.83 microns. Glycerin was employed to minimize the Fresnel reflections otherwise occurring at glass-to-air interfaces; its refractive index closely approximates that of mineral oil, which is employed as a matching fluid and lubricant in the prototype optical penetrators. The insertion loss of the test configuration is plotted in Figure 7 as a function of fiber lateral displacement over a range of symmetrical fiber to lens face setback clearances.

It was observed that the insertion loss was minimized for setbacks on the order of 0-25 micrometers, as would be predicted by equation (3) for a SELFOC lens of 0.499 pitch length ($\ell_1 = \ell_2 = 22$ micrometers). Insertion loss increases rapidly for setbacks exceeding approximately 40 micrometers. Near the optimum setback distance, transverse alignment tolerances are comparable to those observed with butt-coupled fibers, implying that the image of the fiber core is distinct. As the setback distance increases, causing the image to defocus, the tolerances relax somewhat; the larger, blurred image is easier to maintain aligned with the receiving fiber. This indicates a tradeoff between insertion loss and criticality of alignment. Measured insertion loss as a function of setback distance, assuming perfect transverse alignment, is given by Figure 8, for the case of a 0.499 pitch lens immersed in glycerin.

This experiment demonstrates for the case of “perfect” fiber alignment, that the insertion loss of a typical SELFOC relay lens is nominally 0.3 dB under the conditions evaluated. In order to maintain less than 1.0 dB of total insertion loss in a demountable pressure penetrator, the transverse, peak fiber alignment error must be less than 11 micrometers. Longitudinal tolerances of less than 38 micrometers must be maintained. In

the case where a total insertion loss of 3 dB is tolerable, peak tolerances must be less than 22 micrometers and 100 micrometers, respectively.

Because the chromatic dependence of the lens introduces an effect similar to that of altering pitch length as a function of wavelength, the results of Figures 7 and 8 can be employed to estimate the increase in insertion loss due to chromatic aberration. In the case of a penetrator optimized for operation at 0.83 micron, the effect of introducing 1.06 micron light is the same as reducing the pitch length of the rod from 0.498 to 0.491 but not reoptimizing end clearances. This would result in approximately 3-4 dB of additional insertion loss. The magnitude of this effect can be reduced by optimizing the penetrator at a wavelength intermediate to the two wavelengths specified. This tradeoff approach is clearly system dependent because the transmission link may operate with much greater margin at the longer wavelength (this is usually the case), hence, the link may be able to afford greater insertion loss due to the penetrator at the longer wavelength. Fortunately, this effect is much less severe at the longer wavelengths presently contemplated for long-haul, undersea system applications. For example, if the previous wavelengths are changed to 1.27 and 1.55 microns, the increased insertion loss at the longer wavelength is approximately 0.8 dB if the penetrator is optimized at the shorter wavelength. Optimization of the penetrator at an intermediate wavelength would result in even smaller chromatic effects.

MECHANICAL CONSIDERATIONS

In order to predict environmental performance of the penetrator design, it is necessary to determine the mechanical effects due to externally applied stimuli: differential pressure (glass stress, epoxy shear) and temperature cycling (glass compressive stress).

Glass stress was modeled as a function of pressure by considering a circular steel disk with a centrally located 0.080 inch diameter hole to approximate the condition encountered when a SELFOC rod is bonded into a metal bulkhead. This assumption implies that the glass, which would fill the hole in the actual device, exerts no restoring force upon the metal surrounding it. This corresponds to a worst-case assumption insofar as plate deflection is concerned. The plate was assumed to cover a 1-inch diameter mounting bore as depicted in Figure 9.

Results of the modeling are given in Figure 10 for an applied pressure of 10,000 psi. Plate displacement due to flexure, hole radius contraction (at the high pressure surface), and tensile load on the steel plate are plotted vs plate/window thickness.

The failure mode of the glass was hypothesized to be spalling of the edges of the high pressure face of the SELFOC lens due to the uneven compressive forces acting upon the

window as a result of plate flexure under applied pressure. This hypothesis was verified experimentally utilizing a 0.250 inch thick glass window mounted in a type 1704 stainless steel bulkhead using a hard solder sweat. Failure due to spalling of the edges of the window was first observed when the applied pressure exceeded 5000 psi, corresponding to a calculated plate deflection of 0.001 inch, a change in hole radius of 0.0005 inches at the high pressure surface, and a stress level in the steel of 90,000 psi. No leakage occurred at a pressure of 11,500 psi (the limit of our test equipment), even though the high pressure side of the window was badly spalled and glass fractures in planes parallel to the bulkhead had formed. The low pressure side of the window remained intact. Because the bulkhead containing the SELFOC rod in the penetrator design reported here is approximately 0.65 inch thick, window failure at a pressure of 50,000 psi can be inferred from Figure 10 due to glass spalling. Plate deflection corresponds to less than 0.0001 inch at a working pressure of 10,000 psi. Stress upon the steel is only 20,000 psi; this allows for the employment of a low-strength metal alloy selected for free cutting properties and corrosion resistance criteria instead of tensile strength. A safety factor of approximately five at an applied pressure of 10,000 psi is inferred for glass breakage.

The shear force acting upon the epoxy employed to bond the SELFOC rod into the metal bulkhead was calculated using equation 6, derived from geometrical considerations.

$$S = \frac{1}{4} P (d/l) \quad (6)$$

where:

S = Shear force, psi

P = Pressure differential, psi

d = SELFOC lens diameter

l = SELFOC lens length

The aspect ratio (d/l) of a 0.5 pitch SLS SELFOC lens is 0.122, independent of rod diameter. The epoxy employed is Epotec Type 301-2 which is specified as having a lap shear strength (aluminum-to-aluminum) of 2,000 psi. Allowing the epoxy shear strength to be derated to 1,000 psi for the case of glass-to-steel bonding (probably conservative), the epoxy will shear at an applied pressure level of 33,000 psi, corresponding to a safety factor of at least 3-4 for the epoxy bond.

The thermal stress effect was modeled by a 0.080 inch diameter borosilicate crown glass rod in intimate contact with a 2.0 inch diameter concentric stainless steel annulus.

Because the temperature coefficient of the metal is greater than that of glass, the metal is expected to squeeze the glass at cold temperatures, placing it under stress. Under these assumptions, the glass is subjected to a radial compressive loading of 1,030 psi when cooled from +20 C to -20 C (reference 5). This is well below the 50,000 psi compressive strength typical of soft glasses. Because the glass and metal in the penetrator are not actually in intimate contact, but have a thin film of epoxy between them (which has an elastic modulus approximately a factor of 30 less than either the glass or the metal), the above calculation is quite conservative. In practice, the epoxy acts as an elastic cushion layer which effectively reduces compressive and tensile loading upon the glass. The penetrator is expected to pass MIL temperature cycling over the range of -55 G to +125 C in storage at 1 atmosphere. Whether the device can maintain satisfactory operational insertion loss under such conditions and remain within optical specifications is currently under determination.

The mechanical tolerances which must be maintained in order to assure satisfactory optical performance for a demountable fiber optic penetrator (or connector) are quite stringent. In order to achieve less than 1.5 dB of total insertion loss due to misalignment and defocusing, it was determined from Figures 7 and 8 that the following peak mechanical tolerances in locating the fiber cores must be achieved in production and maintained in the field:

Transverse	less than 15 micrometers, or
Concentricity	less than 15 micrometers, or
Longitudinal	less than 60 micrometers.

These tolerances correspond to those required to mate a pair of 50 micron core, graded index telecommunication fibers in an “optically satisfactory” manner. Each tolerance corresponds to a peak value and assumes that all other mechanical misalignment is negligible. For the purpose of this analysis, peak displacement error values are employed; it is assumed that multiple misalignments add in an RMS manner (average errors accumulate). In practice, the possibility exists for poorer (or better) performance because peak values may add (or subtract) constructively. On the average, however, such events appear to be relatively improbable.

The connector selected to mate with the prototype penetrator is the popular, Type 906, as manufactured by Amphenol, Inc. Measurements taken on seven Type 906 connectors indicate that the following peak mechanical tolerances are achieved using field installed, production devices:

Transverse	0 (absorbed into fiber diameter)
Concentricity	3 micrometers
Lapped Length	5 micrometers

Manufacturer's data from International Telephone and Telegraph Corporation and other optical fiber producers, indicate that the tolerances presently achievable with regard to the optical fibers themselves are on the order of:

Transverse (diameter)	5 micrometers
Core concentricity	5 micrometers
Length	0 (if lapped into a connector)

If tolerances for two connectors are combined and added in an RMS fashion, the total error can be estimated for a mated pair of "perfectly aligned" connectors containing installed fibers:

Transverse	10.9 micrometers
Longitudinal	7.1 micrometers

It is seen that under ideal conditions (an absolutely perfect external alignment mechanism is employed to index the connectors) considerably less than 1.5 dB of total insertion loss should be achievable (misalignment less than 15 micrometers). It is also apparent that it is just barely possible (in theory) to achieve the required 11.0 micron peak tolerance (on the average) necessary to exhibit less than 1 dB insertion loss. The above, of course, postulates an alignment mechanism with no error of its own. This cannot be the case, hence, tolerances in the penetrator alignment mechanism (particularly transverse errors), will contribute to overall insertion loss and will begin to dominate if allowed to exceed approximately 10-15 micrometers. Longitudinal tolerance must be held to much less than 60 micrometers if longitudinal misalignment is not to introduce appreciable additional insertion loss. If the longitudinal locating accuracy of the penetrator is better than approximately 5 micrometers, longitudinal errors will be dominated by the length uncertainties of the lapped connectors themselves.

It was determined that the fabrication technique could utilize precision machining operations (turning and lapping) to achieve the required longitudinal alignment accuracy, but that it would be necessary to provide some type of adjustable alignment mechanism

which would be permanently locked into position after adjustment to achieve transverse alignment. This is necessary for metal machining considerations and because the optical axis of the SELFOC lens may not correspond exactly to its physical axis. The design presented in this paper utilizes a movable stainless steel plate accommodating one connector assembly. This connector assembly is slid upon a film of epoxy resin to achieve accurate transverse alignment with the penetrator body containing the SELFOC lens and the other connector. Upon curing, the epoxy locks the entire assembly into a single unit which is permanently aligned. Currently, investigation is underway in an effort to eliminate the use of epoxy for this function due to possible long-term instability and fatigue due to pressure cycling. Electron beam welding is under consideration for joining the alignment plate to the penetrator body in a permanent and stable manner. Likewise, the use of high tin content solder is being investigated to replace epoxy for the function of bonding the GRIN rod into the bulkhead in order to achieve hermeticity.

CONSTRUCTIONAL REALIZATION

Six prototype penetrator units were constructed during FY 80 at NOSC in order to verify the concept presented previously and to provide units for preliminary test and evaluation. An assembly drawing depicting the Construction of the units is given in Figure 11. Construction is of Type 303 alloy stainless steel.

The penetrator units were constructed in two sections: A penetrator body, which provides the sealing, pressure barrier, and imaging functions, and an alignment plate which permits the required transverse tolerances to be achieved. A pressure equalization hole in the alignment plate allows for oil transfer as the connector is inserted or removed from the penetrator. The SELFOC lenses were bonded into the bulkheads using low viscosity epoxy (Epotec 301-2) which was inserted using a vacuum filling technique to ensure that voids were not formed (reference 6). After approximately 48 hours of curing at 30 C, each completed penetrator body assembly was pressurized to 11,500 psi for approximately 1 hour. (Before-and-after dimensional measurements with a precision dial indicator demonstrated that negligible rod movement due to epoxy creep resulted from this proof test.) In a similar manner, the penetrator body can be certified for pressure and shock integrity prior to integration with other optical components such as connectors and cables. A photograph of a prototype penetrator prior to final assembly is shown in Figure 12. An optional indium solder vapor seal can be deposited, bridging glass and metal, if hermeticity is required.

The final assembly process joins the two sections into a complete penetrator assembly. This function is accomplished by X-Y micropositioning the alignment plate (containing an installed Type 906 connectorized fiber) with respect to the penetrator body (containing another such connectorized fiber) in order to maximize the intensity of an optical test

signal which is transmitted through the unit while it is installed in the alignment fixture. A 2.5 pound weight serves to press the alignment plate into close proximity with the penetrator body. The plate floats on a thin film of catalysed epoxy resin, which acts as a lubricant. The epoxy ultimately cures to provide a stable joint which locks the sections together into a unitized penetrator. After the alignment is accomplished but before the epoxy has set, the assembly is tacked together with several drops of cyanoacrylate instant adhesive (Loctite Type 495). The cyanoacrylate creates a stable bond in less than 5 minutes which is strong enough to permit handling of the assembled penetrator without allowing plate movement. This permits the aligned, but uncured, unit to be removed from the alignment fixture for the duration of the epoxy set-up time (approximately 2 days); this frees up the fixture for alignment of other units. Likewise, the technique can be utilized to maintain alignment prior to electron beam welding of the plate and the penetrator body. A completed penetrator is shown in Figure 13.

SUMMARY AND CONCLUSION

A design for and several prototype models of high performance, demountable, high pressure penetrators for fiber optic cables were developed. Such devices will be required to realize practical undersea systems employing fiber optic cables. The approach utilizes the imaging properties of GRIN rod lenses to provide a low insertion loss, high pressure window (which is sealed into the pressure bulkhead). Such an approach overcomes the disadvantages exhibited by previous attempts to realize fiber optic penetrators, which attempted to seal the fiber itself or the entire cable jacket into a bulkhead. The GRIN rod approach preserves essentially all of the operational attributes associated with conventional electrical pressure penetrators, making system design using fiber optic cables in the undersea environment more straightforward. Composite penetrators and connectors containing both fiber optic data transmission elements and electrical power pins are readily implemented using the technique. The realization allows glass-to-metal sealing to be incorporated into the penetrator design for use in conjunction with high-reliability electronic systems.

The prototype penetrators constructed during this program were capable of an optical insertion loss of 0.3 dB in a nondemountable configuration and 1.5 dB when made fully demountable by use of interchangeable optical fiber connectors. In the latter case, the insertion loss was dominated by mechanical imperfections in the presently available connectors and optical fibers. The mechanical tolerances required to machine the penetrator alignment receptacles were found to be obtainable using industry-accepted, precision machining techniques. A unique fine adjustment feature incorporated into the realization relaxes the machining requirements associated with the critical connector transverse alignment specification, making the design readily manufacturable.

Preliminary testing carried out at NOSC (reference 7) has shown the prototype penetrator units capable of withstanding pressures in excess of 10,000 psi with no measurable degradation (this pressure level corresponds to operation with a calculated safety factor of approximately 3 to 4). No damage occurs to the units when cycled between temperatures of -40 C to +100 C. Ongoing testing will characterize optical performance as a function of external stress.

The design presented here appears to be a promising approach for realizing fiber optic undersea penetrators for Navy systems. Desirable operational features traditionally associated with electrical penetrators are readily supported in fiber optic penetrators when GRIN imaging rods are employed as pressure windows. Prototype devices have been shown to exhibit excellent optical and mechanical performance while simultaneously permitting practical manufacturing techniques to be employed for construction.

This work was initiated by Code 013 of the Naval Ocean Systems Center, San Diego, California, as an Independent Exploratory Development effort. Current sponsorship is through the NAVAIR Fiber Optic Block Program.

The author wishes to credit R. Uhrich and C. Young, who performed the mechanical analysis, and J. Daughtry who fabricated the prototype penetrators.

REFERENCES

1. Redfern, J., Taylor, H., Eastley, R., Albares, D. "Fiber Optic Towed Array", NUC TP 414, October 1974, pp. 22-24.
2. Ockert, D. "An Underwater Penetrator Development in Fiber Optics", Oceanic Engineering Report Number 79-23, Westinghouse Oceanic Division, Contract IR&D:78615, 30 April 1979.
3. Redfern, J. "High-Pressure Optical Bulkhead Penetrator", United States Patent 3,825,320, filed 2 March 1973, granted 23 July 1974.
4. Roark, R.J., Formulas for Stress and Strain, McGraw-Hill, NY, 1965.
5. Gatewood, B.C., Thermal Stresses: With Applications to Airplanes, Missiles, Turbines, and Nuclear Reactors, McGraw-Hill, NY, 1965.
6. Cowen, S.J., Daughtry, J.H., Young, C., Redfern, J., "Undersea High Bulkhead Penetrator for use with Fiber Optic Cables", United States Patent, Navy Case No. NOSC-86, filed November 1980.
7. Cowen, S.J., "A High-Performance Optical Fiber Pressure Penetrator for use in the Deep Ocean", NOSC TR 644 of May 1981.

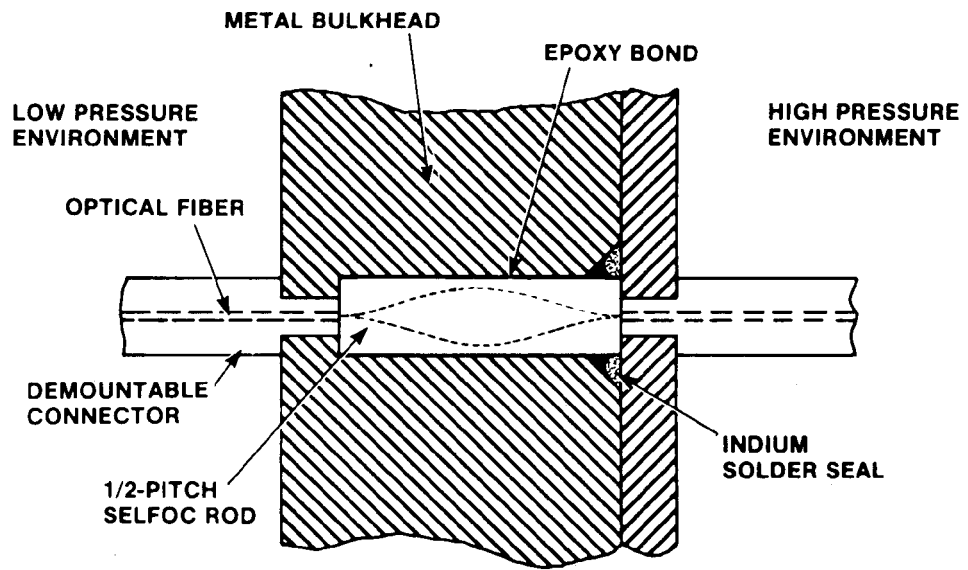


Figure 1 - Schematic - Graded Refractive Index (GRIN) rod lens - combination pressure barrier and imaging device.

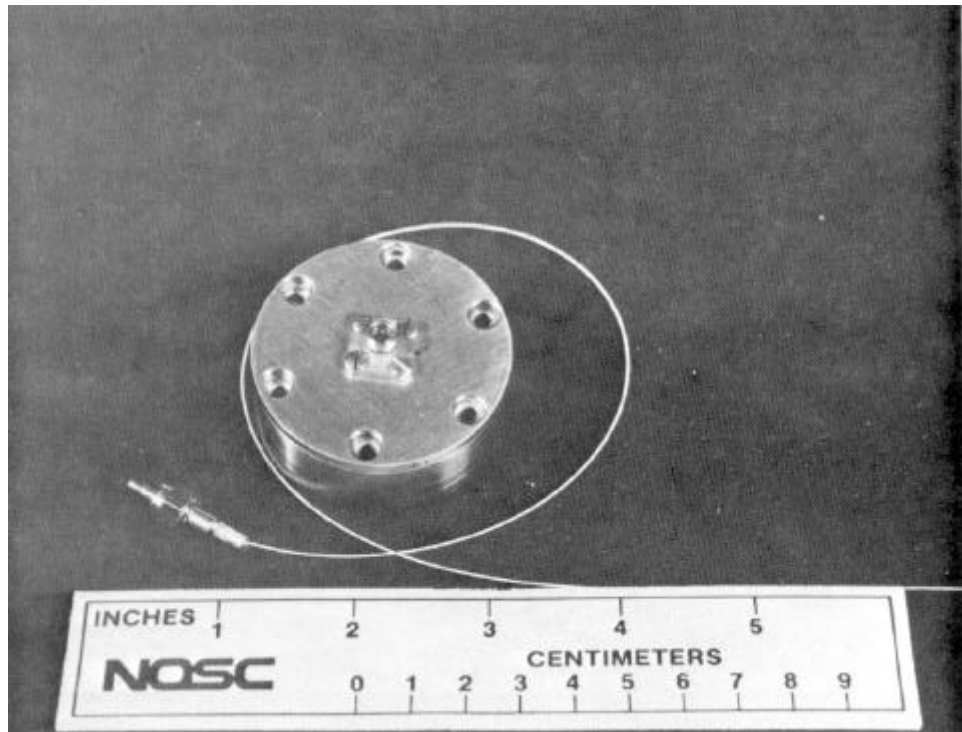


Figure 2 - Prototype Fiber Optic, High Pressure Bulkhead Penetrator.

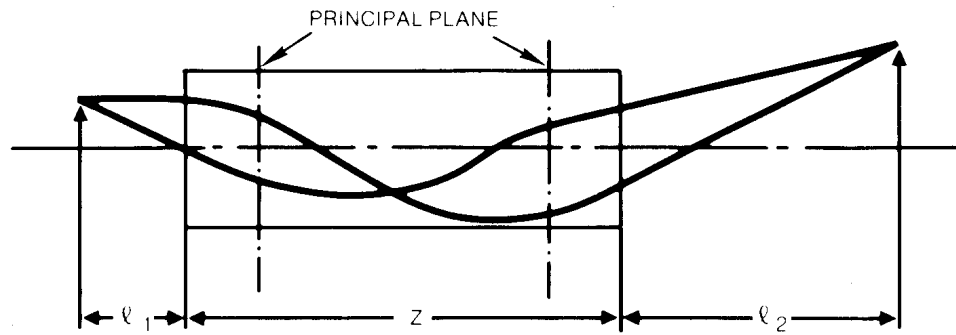


Figure 3 - Ray trace of SELFOC lens immersed in a fluid medium.

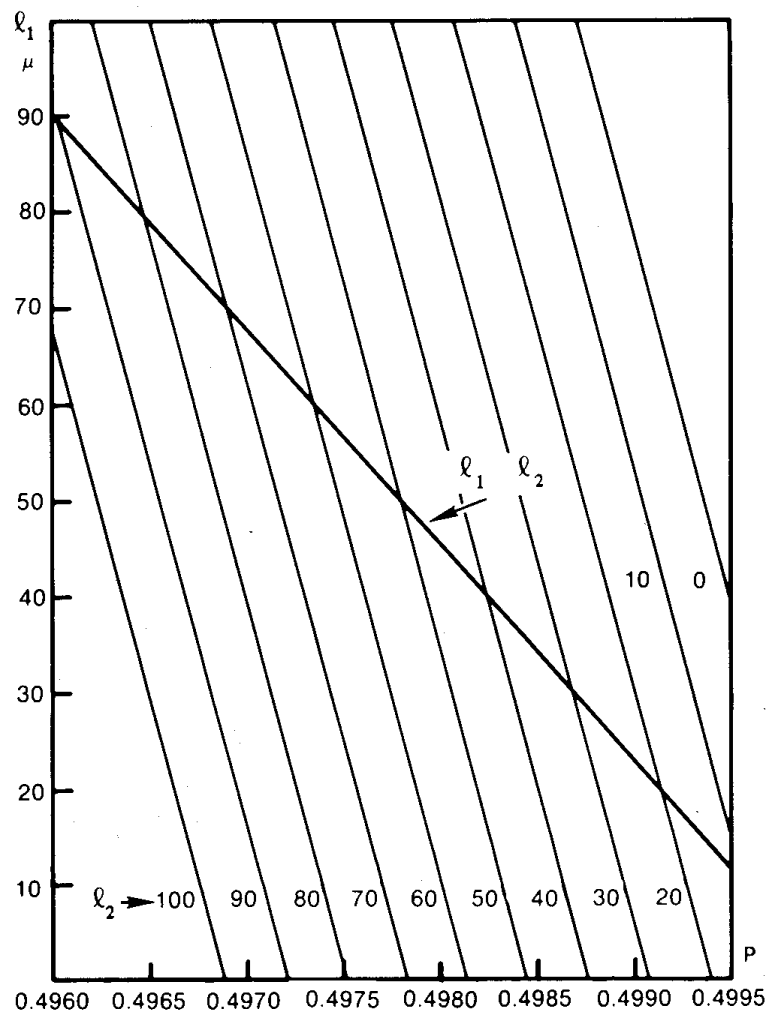


Figure 4 - Parametric plots for the case of symmetrical lens-to-connector spacing conditions.

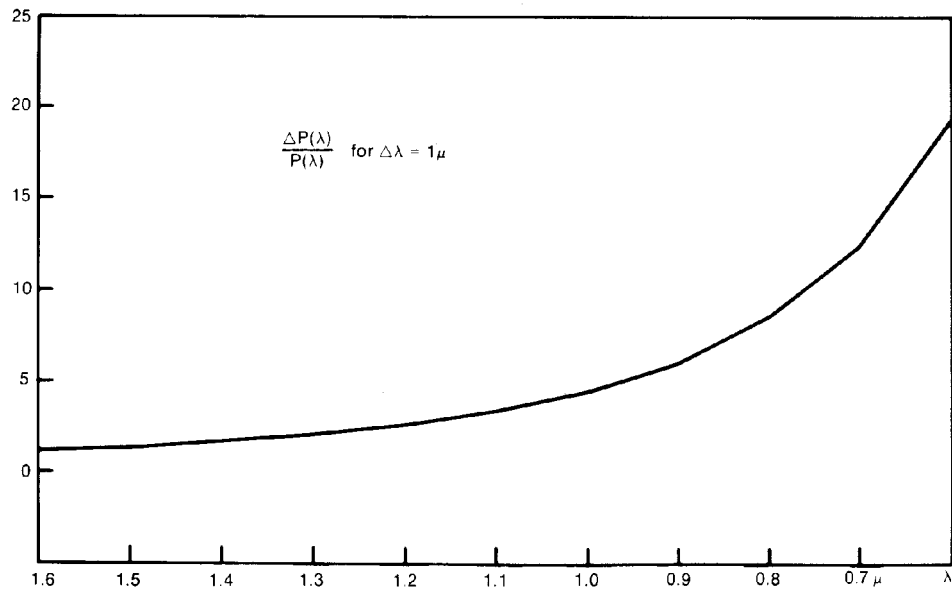


Figure 5 - Chromatic pitch dependence vs wavelength for NSG type SLL/2mm SELFOC rod lens

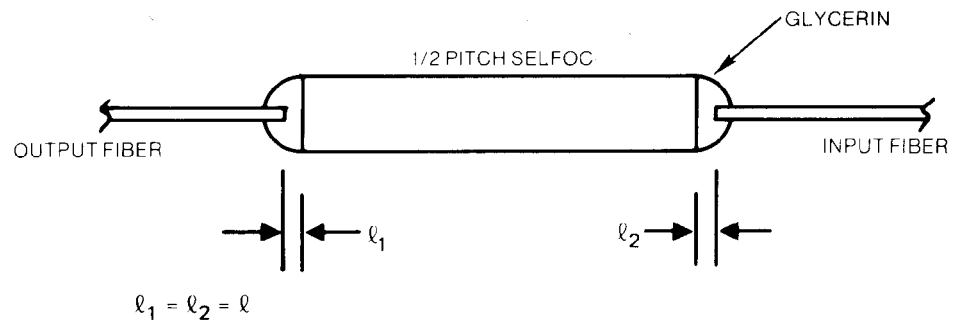


Figure 6 - Experimental configuration employed to evaluate the insertion loss of SELFOC lens.

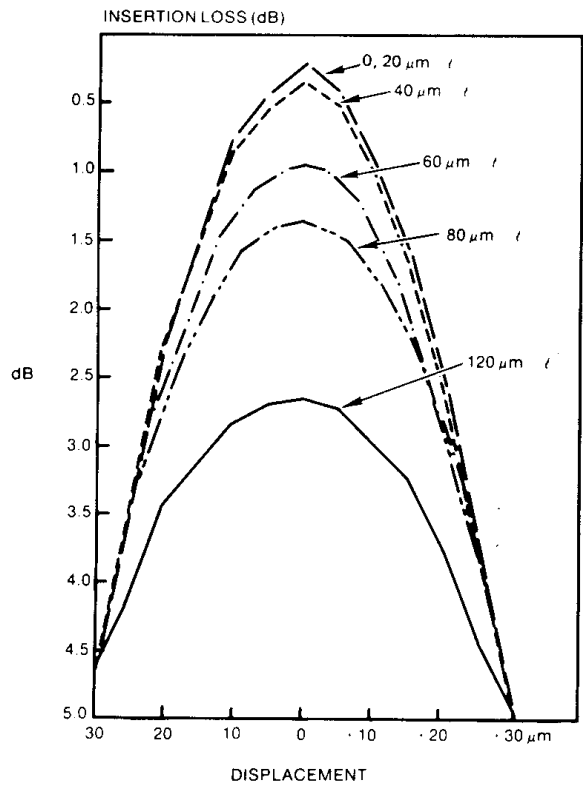


Figure 7 - Transverse displacement loss of optical fibers imaged by 0.499 pitch SELFOC lens.

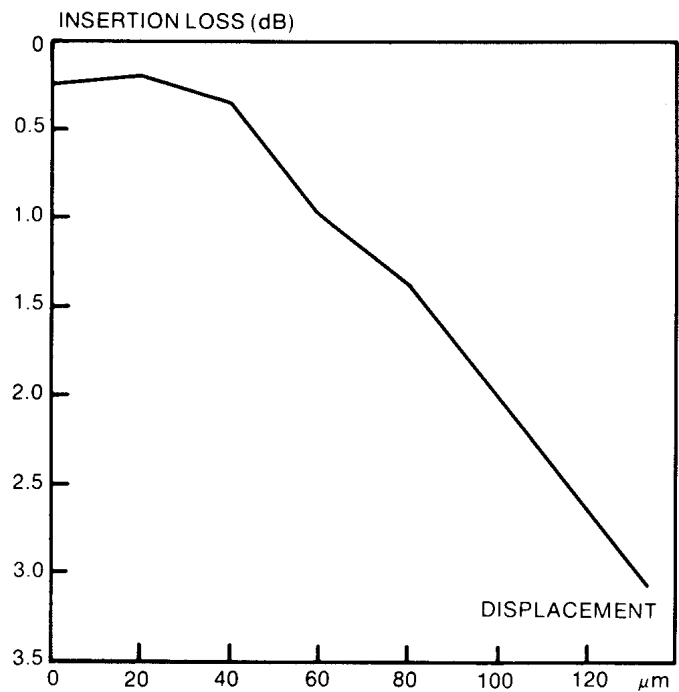


Figure 8 - Longitudinal displacement loss of optical fibers imaged by 0.499 pitch SELFOC lens.

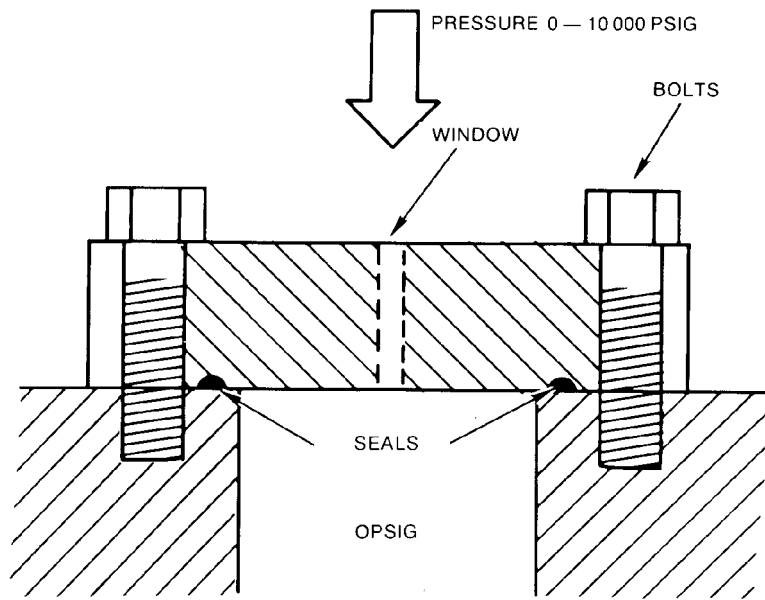


Figure 9 - Plate covering a 1-inch diameter mounting hole, modeling considerations.

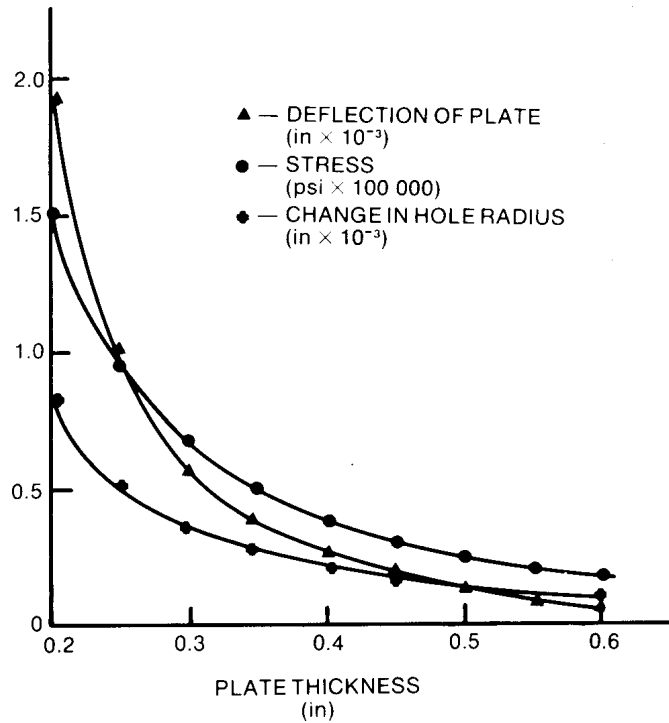


Figure 10 - Results of plate deflection modeling for an applied pressure of 10,000 psi.

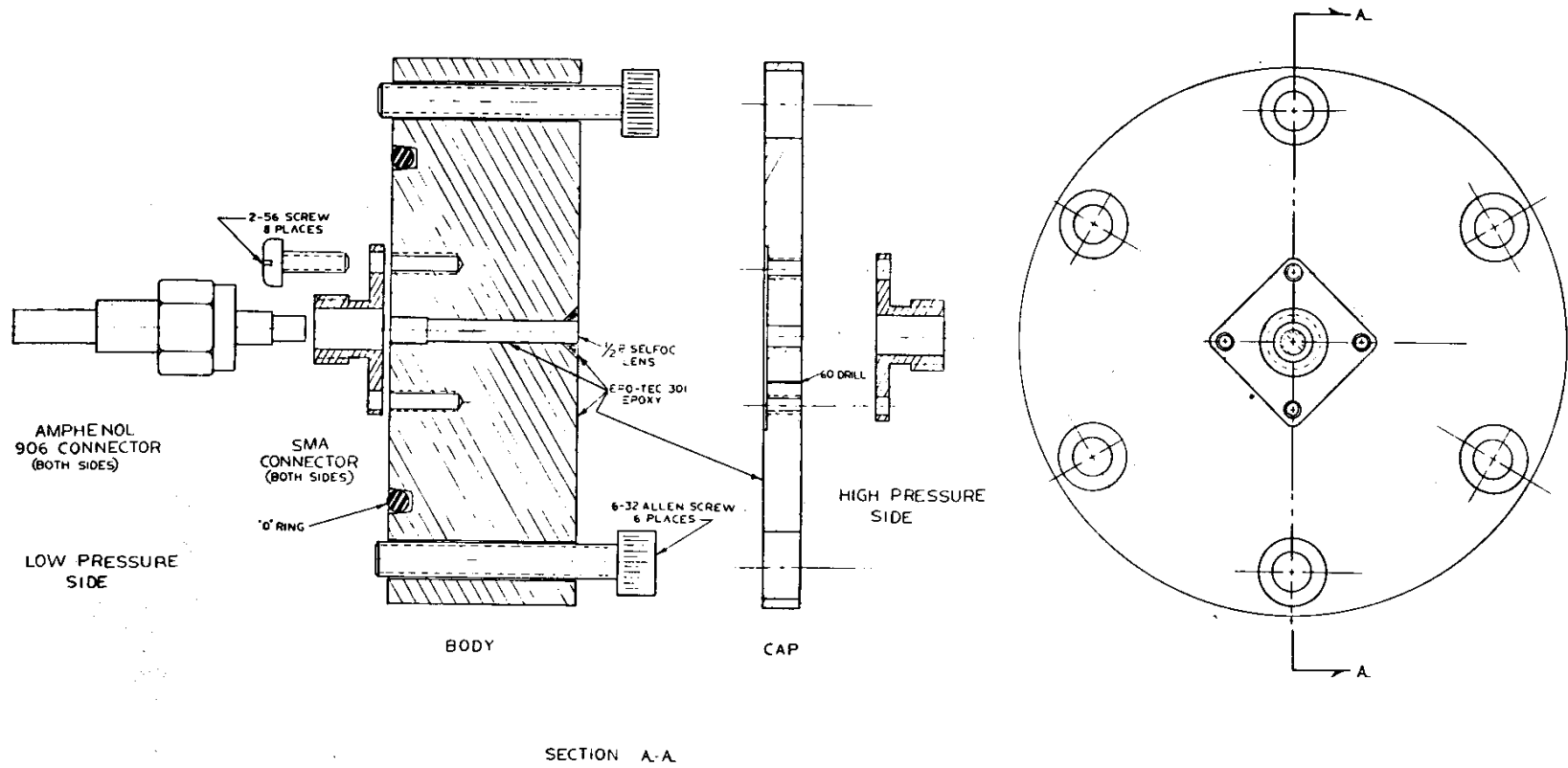


Figure 11 - Fiber Optic penetrator assembly.

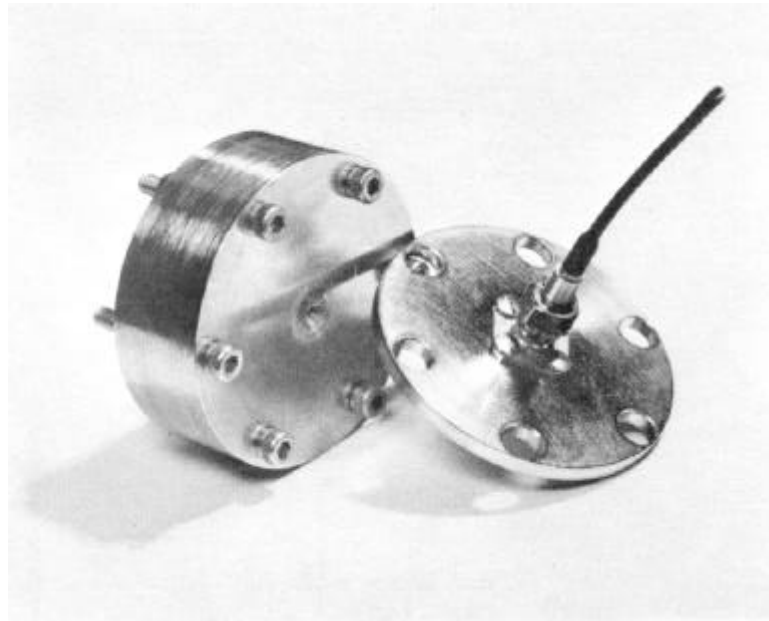


Figure 12 - Fiber Optic bulkhead penetrator prior to final assembly of alignment plate.

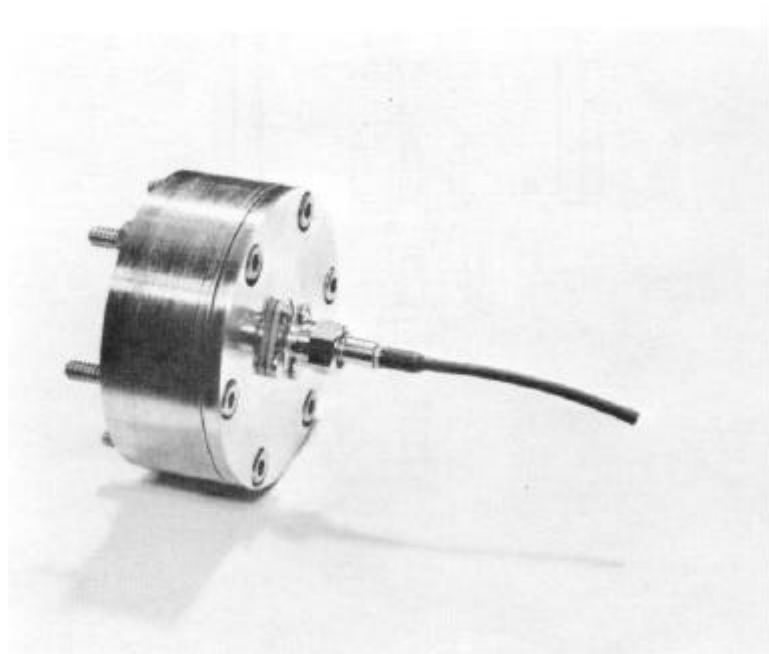


Figure 13 - Assembled Fiber Optic bulkhead penetrator.